Fluorescence Spectroscopic Properties and Crystal Structure of a Series of Donor−Acceptor Diphenylpolyenes

Yoriko Sonoda,*,† Midori Goto,‡ Seiji Tsuzuki,§ and Nobuyuki Tamaoki†

Nanotechnology Research Institute and Technical Center, National Institute of Advanced Industrial Science and Technology (AIST), Higashi 1-1-1, Tsukuba, Ibaraki 305-8565, Japan, and Research Institute of Computational Sciences, National Institute of Advanced Industrial Science and Technology (AIST), Umezono 1-1, Tsukuba, Ibaraki 305-8568, Japan

Received: August 1, 2006; In Final Form: September 12, 2006

A series of *p*-nitro-*p*′-alkoxy(OR)-substituted (*E*,*E*,*E*)-1,6-diphenyl-1,3,5-hexatrienes (**1a**, R = Me; **1b**, R = Et; **1c**, R = *n*-Pr; **1d**, R = *n*-Bu) were prepared. The absorption and fluorescence spectra in solution were almost independent of the alkoxy chain length. The absorption maximum showed only a small dependence on the solvent polarity, whereas the fluorescence maximum red-shifted largely as the polarity increased. The solid-state absorption and fluorescence spectra were red-shifted relative to those in low polar solvents and were clearly dependent on the alkoxy chain length. The fluorescence maxima for the crystals of **1b** and **1d** were observed at 635−650 nm, which were red-shifted by 40−50 nm relative to those for **1a** and **1c**. The Stokes shifts were all relatively small (3000−3500 cm^{-1}). For all four compounds, the fluorescence decay curves in the solid state were able to be analyzed by single-exponential fitting to give the lifetimes of 1.1−1.3 ns. This indicates that the emission of **1a**−**d** is not originated from an excimer or molecular aggregates, but from only one emitting monomeric species. The fluorescence quantum yields of **1a**−**d** were considerably high compared with the values for organic solids, which is consistent with their monomeric origin of emission. Single-crystal X-ray structure analyses of **1a**, **1c**, and **1d** showed that the crystal packing was dependent on the alkoxy chain length. The crystals of **1a** and **1c** had herringbone structure, whereas that of **1d** had π-stacked structure. Strong $\pi-\pi$ interaction in the crystal of **1d** would be the cause of the spectral red shifts relative to those for **1a** and **1c**. No observation of excimer fluorescence from crystal **1d** can be attributed to the limited overlap between the π-planes of the molecules due to its "slipped-parallel" structure.

Introduction

Fluorescent organic solids are attractive due to their potential applications in light emitting diodes (LEDs), solid-state laser dyes, and other photoactive materials.[1,2] Advantages of organic materials over inorganic ones are the ease of fabrication and the tunability of emission properties through a simple chemical modification. Various kinds of organic compounds, which include distyrylbenzene[3−5] and its related molecules,[6,7] fluorenes,[8,9] pentacenes,[10] and pyrenes,[11] have been synthesized, and their solid-state emission properties have been intensively studied up to now.[12−15]

In the use of organic solids as light emitting materials, a major problem is the decrease in fluorescence intensity due to aggregation of molecules, that is, the formation of an excimer-(-like species) and H-type molecular aggregates.[5,13,16] To prevent the aggregation, introduction of an appropriate substituent into a fluorescent molecule has been shown to be effective.[17−19] The introduction of an ethyl group on the conjugated chain of diphenylbutadiene decreases the planarity of the molecules, leading to monomer-like fluorescence in the bulk state.[17] The incorporation of quinacridone dye molecule into dendrimers also decreases molecular aggregation and enhances the emission efficiency in the condensed phase.[18] It has recently been reported that the solid-state emission properties of anthracenesulfonates are controllable by changing the size and shape of countercations, and that monomer emission has been observed in some cases.[20]

Donor−acceptor (D−A) (intramolecular charge transfer (ICT)) molecules are one of the most important classes of compounds for organic materials exhibiting red fluorescence emission.[21,22] Therefore it is expected that, if we introduce appropriate substituents into D−A compounds, we can obtain solid-state materials emitting red-shifted, strong fluorescence due to monomeric species. In contrast to numerous studies on the fluorescence properties of D−A compounds in solution,[21,23−26] however, reports on their emission properties in the solid state have been very limited.[6,19,22,27] The possibility of monomer emission is, of course, strongly dependent on the crystal structure. However, the relationship between the crystal structure and the solid-state emission property for D−A compounds is not fully understood at present.

(*E*,*E*,*E*)-1,6-Diphenyl-1,3,5-hexatriene (DPH) is known to be a highly fluorescent molecule with a linear polyenic structure, and is commercially available as a fluorescence probe in biochemical membrane studies. We have previously reported that the solid-state fluorescence properties of symmetrically ring-substituted DPHs were strongly dependent on the electron-donating/-accepting nature of substituents.[28] Considering the rodlike structure of DPH, it is expected that the D−A substitution on its aromatic rings leads to strong ICT in the ground and

* Corresponding author. Fax: +81-29-861-4673. E-mail: y.sonoda@aist.go.jp.
† Nanotechnology Research Institute.
‡ Technical Center.
§ Research Institute of Computational Sciences.

10.1021/jp064937j CCC: $33.50
Published on Web 11/23/2006

SCHEME 1

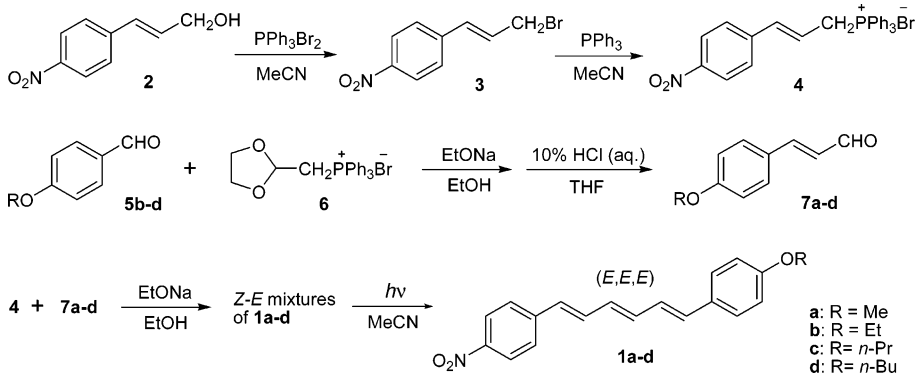

excited states. In our brief study on the photochemical behavior of *p*-nitro-*p*′-methoxy-substituted DPH in solution, we have found that its *Z*,*E* photoisomerization was inefficient in acetonitrile, probably due to the formation of a photochemically inactive CT excited state.[29]

Nitroalkoxy-substituted DPHs with alkoxy chains of different lengths can easily be obtained by Wittig reactions from corresponding alkoxy-substituted cinnamaldehydes and the phosphonium salt of nitrocinnamyl bromide. It is known that the solid-state fluorescence properties of one-dimensional π-conjugated molecules such as DPH are strongly dependent on the coplanarity of conjugated systems and on the distance of conjugated chains.[2] The introduction of alkoxy chains with different lengths into the DPH framework should change the arrangement of the π-systems in the crystal space, and should consequently heavily affect the emission properties in the solid state.

In this study, a series of D−A-substituted (*E*,*E*,*E*)-DPHs, **1a**−**d** (Scheme 1), were prepared. Their solid-state absorption and emission properties and crystal structures were systematically investigated. These compounds were all photochemically stable in the solid state.

Experimental Section

Materials. 4-Nitrocinnamyl alcohol (**2**), 4-alkoxybenzaldehydes (**5b**−**d**), (1,3-dioxolan-2-yl)methyltriphenylphosphonium bromide (**6**), and (*E*)-4-methoxycinnamaldehyde (**7a**) were purchased from TCI and used without further purification. 4-Alkoxycinnamaldehydes **7b**−**d** were prepared from **5b**−**d** and **6** according to the litarature.[30] Pyrene (optical grade) was purchased from Fulka and used as received. All solvents used in the measurements of absorption and fluorescence spectra were of spectroscopic grade (Dojin).

Characterization. High-resolution mass spectra were obtained using a Hitachi M-80B instrument. IR spectra were recorded on a Mattson Infinity Gold FT-IR spectrometer. ^{1}H and ^{13}C NMR spectra were recorded on a Varian Gemini-300 BB spectrometer (300.1 MHz for ^{1}H and 75.5 MHz for ^{13}C) with tetramethylsilane (TMS) as internal reference.

(*E*,*E*,*E*)-1-(4-Methoxyphenyl)-6-(4-nitrophenyl)-1,3,5-hexatriene (1a). To a solution of **4** (0.61 g, 1.2 mmol) and **7a** (0.19 g, 1.2 mmol) in ethanol (8 mL) was added a solution of sodium ethoxide in ethanol (0.30 M, 4 mL). The mixture was stirred under nitrogen atmosphere at 40 °C for 20 h. The resulting orange precipitate was filtered off, washed with water (15 mL) and aqueous ethanol (60%, 20 mL), and dried. The crude product was a 1:1 mixture of *E*,*E*,*E* and *E*,*Z*,*E* isomers of **1a**. The mixture was dissolved in acetonitrile and the solution was irradiated through Pyrex glass with a 500 W high-pressure mercury lamp to induce *E*,*Z*,*E* to *E*,*E*,*E* photoisomerization. After evaporation of the solvent, the resulting gold-orange solid **1a** was purified by recrystallization from toluene. Yield 60%. mp 183−184 °C. MS Found: M^+, 307.1172. Calcd for $C_{19}H_{17}NO_3$: M, 307.1206. ν_{max} (KBr) 3116, 3016, 2983, 2951, 2940, 2865, 1598, 1581, 1521, 1509, 1462, 1344, 1304, 1248, 1175, 1142, 1109, 1022, 1003, 892, 868, 831, 807, 747, and 690 cm^{-1}. ^{1}H NMR ($CDCl_3$) δ 8.17 (2H, d, J = 8.9, arom), 7.51 (2H, d, J = 8.9, arom), 7.38 (2H, d, J = 8.7, arom), 7.03 (1H, apparently (app) dd, J = 15.5 and 10.5, triene), 6.88 (2H, d, J = 8.8, arom), 6.78 (1H, app dd, J = 15.4 and 10.1, triene), 6.44−6.66 (4H, m, triene), 3.83 (3H, s, OCH_3). ^{13}C NMR ($CDCl_3$) δ 161.6, 146.3, 144.1, 137.1, 134.5, 133.9, 131.4, 129.8, 129.2, 127.9, 126.6, 126.5, 124.2, 114.2, 55.3. UV−vis λ_{max} (MeCN) 412 nm (ϵ = 60 800). Single crystals of **1a** for X-ray analysis were obtained by very slow evaporation of acetonitrile solvent at room temperature in the dark.

(*E*,*E*,*E*)-1-(4-Ethoxyphenyl)-6-(4-nitrophenyl)-1,3,5-hexatriene (1b). Triene **1b** was prepared from **4** and **7b** by a procedure similar to that for **1a**. Recrystallization from toluene. Yield 56%. mp 168−170 °C.MS Found: M^+, 321.1363. Calcd for $C_{20}H_{19}NO_3$: M, 321.1363. ν_{max} (KBr) 3117, 3018, 2991, 2941, 2916, 2868, 1600, 1581, 1507, 1477, 1337, 1300, 1244, 1175, 1144, 1109, 997, 889, 867, 826, 801, 746, and 688 cm^{-1}. ^{1}H NMR ($CDCl_3$) δ 8.17 (2H, d, J = 8.8, arom), 7.51 (2H, d, J = 8.8, arom), 7.37 (2H, d, J = 8.7, arom.), 7.03 (1H, app dd, J = 15.5 and 10.5, triene), 6.86 (2H, d, J = 8.7, arom), 6.78 (1H, app dd, J = 15.3 and 10.2, triene), 6.44−6.67 (4H, m, triene), 4.05 (2H, q, J = 7.0, OCH_2), 1.45 (3H, t, J = 7.0, CH_3). ^{13}C NMR ($CDCl_3$) δ 159.1, 146.4, 144.1, 137.2, 134.6, 133.9, 131.3, 129.7, 129.2, 127.9, 126.5, 126.4, 124.2, 114.8, 63.5, 14.8. UV−vis λ_{max} (MeCN) 412 nm (ϵ = 48 700).

(*E*,*E*,*E*)-1-(4-*n*-Propoxyphenyl)-6-(4-nitrophenyl)-1,3,5-hexatriene (1c). Triene **1c** was prepared from **4** and **7c** by a procedure similar to that for **1a**. Recrystallization from toluene. Yield 47%. mp 158−160 °C. MS Found: M^+, 335.1515. Calcd for $C_{21}H_{21}NO_3$: M, 335.1520. ν_{max} (KBr) 3116, 3016, 2970, 2939, 2867, 1599, 1580, 1519, 1510, 1465, 1341, 1300, 1247, 1174, 1143, 1108, 1001, 974, 889, 870, 829, 806, 747, and 690 cm^{-1}. ^{1}H NMR ($CDCl_3$) δ 8.18 (2H, d, J = 8.8, arom), 7.52 (2H, d, J = 8.9, arom), 7.37 (2H, d, J = 8.8, arom), 7.04 (1H, app dd, J = 15.5 and 10.5, triene), 6.88 (2H, d, J = 8.8, arom), 6.79 (1H, app dd, J = 15.3 and 10.2, triene), 6.45−6.68 (4H, m, triene), 3.95 (2H, t, J = 6.6, OCH_2), 1.77−1.88 (2H, m, CH_2Me), 1.05 (3H, t, J = 7.4, CH_3). ^{13}C NMR ($CDCl_3$) δ 159.3, 146.4, 144.2, 137.2, 134.6, 133.9, 131.3, 129.6, 129.1, 127.9, 126.5, 126.4, 124.2, 114.8, 69.6, 22.6, 10.5. UV−vis λ_{max} (MeCN) 413 nm (ϵ = 46 800). Single crystals of **1c** for X-ray analysis were obtained by very slow evaporation of dichlo-

romethane−toluene (7:3 v/ v) mixed solvent at room temperature in the dark.

(*E*,*E*,*E*)-1-(4-*n*-Butoxyphenyl)-6-(4-nitrophenyl)-1,3,5-hexatriene (1d). Triene **1d** was prepared from **4** and **7d** by a procedure similar to that for **1a**. Recrystallization from toluene. Yield 42%. mp 159−161 °C. MS Found: M^+, 349.1663. Calcd for $C_{22}H_{23}NO_3$: M, 349.1676. ν_{max} (KBr) 3115, 3026, 3018, 2960, 2938, 2904, 2870, 1598, 1578, 1509, 1333, 1299, 1243, 1177, 1148, 1106, 1043, 987, 950, 884, 865, 817, 799, 746, and 686 cm^{-1}. ^1H NMR ($CDCl_3$) δ 8.17 (2H, d, $J = 8.9$, arom), 7.51 (2H, d, $J = 8.8$, arom), 7.36 (2H, d, $J = 8.8$, arom), 7.03 (1H, app dd, $J = 15.5$ and 10.5, triene), 6.87 (2H, d, $J = 8.8$, arom.), 6.78 (1H, app dd, $J = 15.2$ and 10.2, triene), 6.44−6.67 (4H, m, triene), 3.98 (2H, t, $J = 6.5$, OCH_2), 1.73−1.82 (2H, m, CH_2Et), 1.43−1.56 (2H, m, CH_2Me), 0.98 (3H, t, $J = 7.4$, CH_3). ^{13}C NMR ($CDCl_3$) δ 159.3, 146.4, 144.1, 137.2, 134.6, 133.9, 131.2, 129.6, 129.1, 127.9, 126.5, 126.4, 124.2, 114.8, 67.8, 31.3, 19.2, 13.8. UV−vis λ_{max} (MeCN) 413 nm ($\epsilon = 50\,600$). Single crystals of **1d** for X-ray analysis were obtained by very slow evaporation of acetonitrile solvent at room temperature in the dark.

Measurements of Absorption Spectra. Absorption spectra in solution were measured in air at room temperature using a Shimadzu UV-3150 spectrometer. Absorption spectra in the solid state were measured in a reflectance mode. The diffuse reflectance spectra were recorded on a Jasco V-560 spectrometer equipped with an integrating sphere accessory (Model ISV-469), using a fluorescence cut filter (HOYA, U-330). The sample solids were placed between quartz plates (40 × 10 mm^2).

Measurements of Fluorescence Spectra, Fluorescence Quantum Yields, and Fluorescence Lifetimes. The corrected fluorescence and excitation spectra of **1a**−**d** in solution and in the solid state were measured in air at room temperature using a SPEX Fluorolog-3 spectrometer. For the fluorescence measurements in solution, the excitation wavelength (λ_{ex}) was set at 420 nm. Concentration of the sample solutions was (1.0−1.5) × 10^{-6} M. Values of fluorescence quantum yield (ϕ_f) of **1a**−**d** in solution were determined using a solution of **1a** in toluene as a standard ($\phi_f = 0.626$). The value of ϕ_f for **1a** in toluene was obtained using a solution of *p*,*p*′-dicyano-substituted DPH in toluene as a standard ($\phi_f = 0.88$, $\lambda_{ex} = 390$ nm).[31] Fluorescence spectra of the crystalline samples were recorded by using the front face geometry. The sample crystals were placed between quartz plates (40 × 10 mm^2) on the sample holder. For all compounds, λ_{ex} was set at 480 nm. Values of ϕ_f in the solid state were estimated by comparison of fluorescence peak areas for the thick microcrystalline samples of **1a**−**d** with that for pyrene ($\phi_f = 0.64$ at 293 K).[32] Fluorescence decay curves in solution and in the solid state were obtained by the time-correlated single-photon-counting method, using a HORIBA NAES 700 equipped with a subnanosecond nitrogen laser system ($\lambda_{ex} = 337$ nm). The monitor wavelength was set at the fluorescence emission maximum (λ_f) shown in Tables 2 and 3 for each compound. The sample solutions were highly diluted. For the solid-state measurements, the sample crystals were placed between quartz plates (40 × 10 mm^2) on the sample holder.

Single-Crystal X-ray Structure Analyses. The single-crystal X-ray diffraction (XRD) measurements of **1a**, **1c**, and **1d** were performed at 183 K using a CCD area-detector diffractometer with graphite monochromated Mo Kα radiation ($\lambda = 0.710\,73$ Å). Data collection, reduction, and empirical absorption correction were carried out using SMART (Bruker, 2001), SAINT-PLUS (2001), and SADABS (2001).[33] The structure was solved by direct methods using SIR92[34] and refined by full matrix least-squares on F^2 with SHELXTL.[35] The non-hydrogen atoms were refined anisotropically. Hydrogen atoms were placed in geometrically calculated positions and refined by use of a riding model.

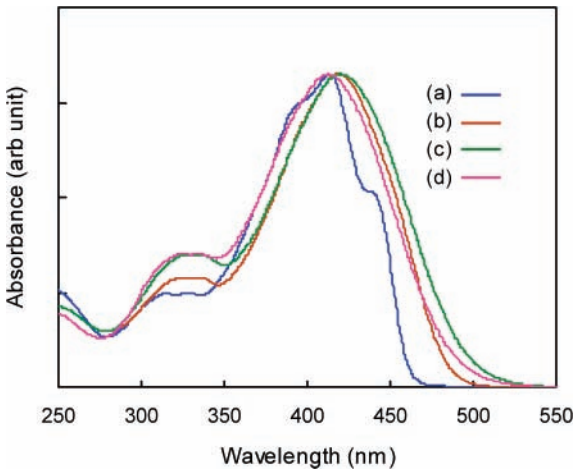

Figure 1. Absorption spectra of **1a** in (a) methylcyclohexane, (b) toluene, (c) dichloromethane, and (d) acetonitrile.

TABLE 1: Absorption and Fluorescence Data of 1a in Solution

solvent	λ_a (nm)	λ_f (nm)	ΔE_{ss} (cm^{-1})	ϕ_f	τ_s (ns)
methylcyclohexane	413	485	3595	0.21	0.70
toluene	419	541	5382	0.63	1.5
dioxane	415	565	6397	0.57	1.9
tetrahydrofuran	417	611	7614	0.44	1.7
chloroform	421	681	9069	0.14	
dichloromethane	420	694	9400	0.074	
dimethyl sulfoxide	429	744	9869	0.030	
acetonitrile	412	740	10758	0.013	
methanol	411	690	9838	0.002	

Powder XRD Pattern Measurement. The powder XRD pattern of **1b** was obtained using a Rigaku RAX-01 diffractometer with graphite monochromated Cu Kα radiation. The cell parameters were calculated using the Xpress program (Mac Science Co., Ltd., 1998).

Computational Method. The Gaussian 03 program was used for ab initio molecular orbital calculations.[36] The geometry of **1a** was optimized at the HF/6-31G* level. The optimized geometry was used for the calculations of energy levels of orbitals and for the CIS calculations of excitation energies.[37] Energy levels of orbitals were calculated at the B3LYP/6-311G** level.[38,39]

Results and Discussion

Absorption and Fluorescence Properties of 1a−d in Solution. *Absorption Spectra in Solution.* Table 1 summarizes the absorption and fluorescence data of **1a** in various solvents. The absorption spectra of **1a** in selected solvents are shown in Figure 1. The absorption maxima (λ_a) were observed in the wavelength range of 411−429 nm and showed only a small dependence on the solvent polarity. The spectrum had vibrational structure in nonpolar methylcyclohexane, while in acetonitrile it was broad and structureless probably due to strong solvent−solute interactions in polar solvents.

Table 2 summarizes the absorption and fluorescence data of **1a**−**d** in some different kinds of solvents. The absorption spectrum in solution was independent of the alkoxy chain length.

In the spectra of **1a**−**d**, two absorption bands were observed around 325 and 415 nm in all solvents studied. To understand

TABLE 2: Absorption and Fluorescence Data of 1a−d in Solution

	solvent											
	methyl-cyclohexane			toluene				dichloromethane			acetonitrile		
compd	λ_a[a]	λ_f[b]	ϕ_f	λ_a	λ_f	ϕ_f	τ_s[c]	λ_a	λ_f	ϕ_f	λ_a	λ_f	ϕ_f
1a	413	485	0.21	419	541	0.63	1.5	420	694	0.074	412	740	0.013
1b	414	488	0.22	419	545	0.50	1.5	420	697	0.068	412	738	0.017
1c	414	488	0.25	420	546	0.54	1.6	421	699	0.060	413	747	0.011
1d	414	488	0.25	420	546	0.53	1.7	421	701	0.060	413	740	0.014

[a] λ_a values in nm. [b] λ_f values in nm. [c] τ_s values in ns.

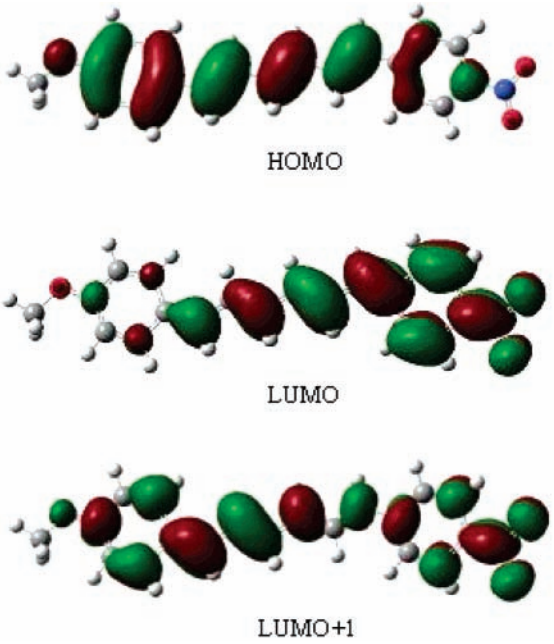

Figure 2. Calculated HOMO, LUMO, and LUMO+1 orbitals of **1a**.

the energy levels and to explain the transitions of these bands, quantum chemical calculations were performed for **1a**. Energies of the HOMO, LUMO, and LUMO+1 were calculated (Supporting Information, Tables S1 and S2). The calculated energy gaps were $\Delta E_{HOMO-LUMO} = 3.02$ eV (411 nm) and $\Delta E_{HOMO-LUMO+1} = 3.97$ eV (312 nm) using B3LYP/ 6-311G**, which agreed well with the experimental values obtained from the UV−vis absorption spectrum (Figure 1). Figure 2 shows the HOMO, LUMO, and LUMO+1 orbitals in the optimized structure of **1a**. The HOMO and LUMO+1 orbitals are delocalized over the whole of the molecule, whereas the LUMO mainly locates on the *p*-nitrophenyl group. Therefore, a significant ICT occurs associated with the HOMO−LUMO transition, which corresponds to the absorption observed around 415 nm. The HOMO−LUMO+1 absorption around 325 nm is attributed to the $\pi-\pi^*$ transition.

Fluorescence Properties in Solution. (a) Fluorescence Spectra in Solution. The fluorescence spectrum of **1a** was strongly dependent on the solvent polarity (Table 1). Figure 3 shows the fluorescence spectra of **1a** in various solvents. As the solvent polarity increased, the position of λ_f shifted largely to longer wavelengths and the spectrum became structureless.

The stronger solvent dependence of the emission spectrum than that of the absorption spectrum, which resulted in the very large Stokes shifts (ΔE_{ss}) in polar solvents (Table 1), suggests an excited state with much stronger ICT character and a large dipole moment relative to those in the ground state. In polar solvents, the ICT excited state is highly stabilized by solvent−solute dipole−dipole interaction, and is responsible for the red-shifted emission. This state would correspond to a twisted ICT ("TICT") state.[31,40]

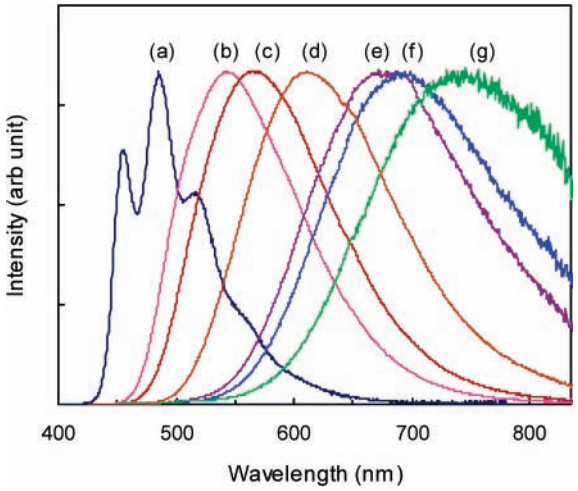

Figure 3. Fluorescence spectra of **1a** in (a) methylcyclohexane, (b) toluene, (c) dioxane, (d) tetrahydrofuran, (e) chloroform, (f) dichloromethane, and (g) acetonitrile. Excitation wavelength: 420 nm.

The fluorescence spectrum was almost independent of the alkoxy chain length in all solvents studied, as in the case of the absorption spectrum (Table 2). Thus, the molecules of **1a−d** behaved as essentially the same chromophores and fluorophores in solution. This is quite reasonable because the absorption and fluorescence emission in diluted solution are monomeric properties of these compounds.

(b) Fluorescence Quantum Yields and Lifetimes in Solution. In low and moderately polar solvents such as toluene and dioxane, ϕ_f values for **1a** were considerably high (Table 1). However, ϕ_f strongly decreased as the solvent polarity increased. A similar trend was observed for **1b−d**. The low ϕ_f in polar acetonitrile and dimethyl sulfoxide suggest highly efficient nonradiative decay from the low-energy ICT excited state.[40]

The fluorescence decay curves of **1a** in low and moderately polar solvents were able to be fitted by a single-exponential function. The obtained fluorescence lifetimes (τ_s) are shown in Table 1. In polar solvents such as dichloromethane and acetonitrile, τ_s's were shorter than the time resolution of our single-photon-counting apparatus. Also, it is possible that the ϕ_f values in these solvents were too small for τ_s measurements. The values of τ_s in toluene for **1a−d** were not greatly different (Table 2).

(c) Fluorescence Properties in Methanol. Although the absorption spectrum of **1a** in methanol was very similar to that in acetonitrile, the fluorescence spectrum in methanol was blue-shifted by 50 nm compared to that in acetonitrile (Table 1). In addition, ϕ_f in methanol was significantly lower than the values in other polar solvents. Considering that methanol and acetonitrile are similar in polarity, the observed unusual behavior of **1a** in methanol suggests that, along with the dipole−dipole interactions between solute and solvent, intermolecular hydrogen bonding may have an influence on its emission properties in methanol.

Solid-State Absorption and Fluorescence Properties of 1a−d. *Absorption Spectra in the Solid State.* Table 3 summarizes the absorption and fluorescence data of **1a−d** in the solid state. Figure 4 shows the solid-state absorption spectra of **1a−d**. For all compounds, the absorption spectra in the solid state were red-shifted relative to those in solution.

In contrast to the case in solution, the solid-state absorption spectrum was dependent on the length of the alkoxy chain. The

TABLE 3: Absorption and Fluorescence Data of 1a−d in the Solid State

compd	λ_a (nm)	λ_a^{onset} (nm)	λ_f (nm)	ΔE_{ss}[a] (cm^{-1})	ϕ_f	τ_s (ns)
1a	505	586	595	2995	0.1−0.2	1.2
1b	525	621	635	3300	0.05−0.1	1.1
1c	501	605	598	3238	0.2−0.4	1.1
1d	531	643	650	3448	0.2−0.4	1.3

[a] Calculated from λ_a and λ_f.

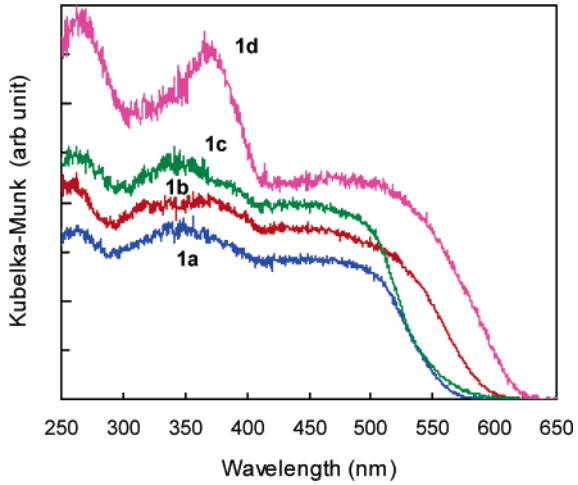

Figure 4. Absorption spectra of **1a**−**d** in the solid state.

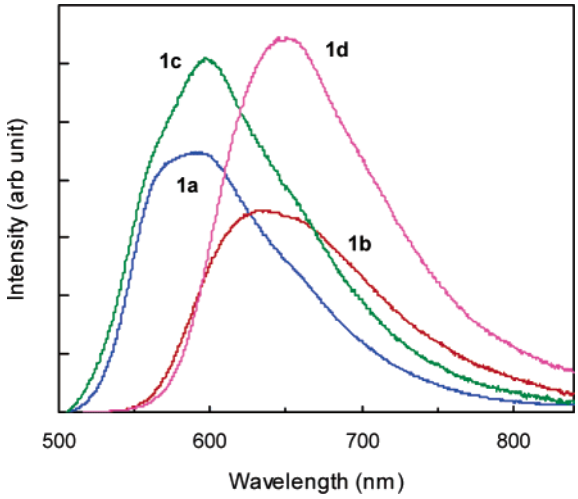

Figure 5. Fluorescence spectra of **1a**−**d** in the solid state. Excitation wavelength: 480 nm.

absorption spectra of **1b** and **1d** were observed at longer wavelengths by 20−30 nm than those of **1a** and **1c**. The difference in absorption energy between **1a** and **1d** was calculated to be 970 cm^{-1} from λ_a and 1513 cm^{-1} from the absorption onset (λ_a^{onset}) (Table 3). Correspondingly, the crystal colors of **1b** and **1d** were orange and orange-red, respectively, whereas those of **1a** and **1c** were yellow.

Fluorescence Properties in the Solid State. (a) Solid-State Fluorescence Spectra. Figure 5 shows the fluorescence spectra for the crystals of **1a**−**d**. The positions of λ_f for **1b** and **1d** were observed at longer wavelengths than those for **1a** and **1c** by 40−50 nm (Table 3). The difference in emission energy between **1a** and **1d** was calculated from λ_f to be 1422 cm^{-1}. The solid-state fluorescence spectrum was thus found to be clearly dependent on the alkoxy chain length, although the energy differences among them were not very large. The excitation spectra of **1a**−**d** were very similar to their solid-state

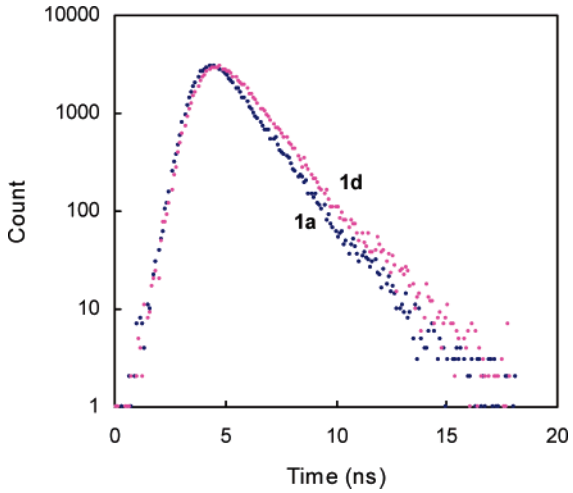

Figure 6. Fluorescence decay curves for the crystals of **1a** and **1d**. Excitation wavelength: 337 nm. Monitor wavelength: λ_f for each compound shown in Table 3.

absorption spectra, and the fluorescence spectrum showed no dependence on the excitation wavelength. From λ_a and λ_f, ΔE_{ss} values for **1a**−**d** were calculated to be 3000−3500 cm^{-1}.

(b) Fluorescence Lifetimes and Quantum Yields in the Solid State. Figure 6 shows the fluorescence decay curves for the crystals of **1a** and **1d**. The decay curves were able to be analyzed by single-exponential fitting for all four compounds. The obtained τ_s values were within the range of 1.1−1.3 ns (Table 3), which are typical values for small organic dye molecules.[2] The values of τ_s for **1a**−**d** were not significantly different. Fluorescence emission from organic solids often shows a multiexponential decay behavior due to efficient migration of excitation energy in the solid state. In the present case, however, fluorescence from crystals **1a**−**d** was found to be single component. This indicates that the emission of **1a**−**d** is originated from only one emitting monomeric species, and that an excimer or aggregated complexes are not involved in the emission processes.[9,41] This assignment is consistent with the relatively small values of ΔE_{ss}.

Although ϕ_f values for organic crystals are, in general, difficult to determine precisely due to the intrinsic inhomogeneity of solid samples, the values for the crystals of **1a**−**d** were roughly estimated using pyrene as a standard. The results are shown in Table 3. The obtained ϕ_f values were considerably large compared with the values for organic solids, in agreement with their monomeric origin of emission.

The small ΔE_{ss} and large ϕ_f values for every crystal also indicate that TICT is not taking place during the photoprocess.

Crystal Structures. *Single-Crystal X-ray Structure Analyses.* Table 4 shows the crystal data of **1a**, **1c**, and **1d** obtained by X-ray structure analyses. The ORTEP representations of the molecular structures are displayed in the Supporting Information. Compound **1b** crystallized into orange needles; however, crystals suitable for X-ray structure analysis have not been obtained at present.

(a) Crystal Structure of **1a**. Crystal **1a** has herringbone structure as shown in Figure 7. Two crystallographically independent molecules (A and B in Figure 7a) exist in a unit cell. The two molecules are nearly planar. The mean deviations from the least-squares plane defined by the DPH moiety are 0.10 and 0.07 Å for A and B, respectively. As shown in Figure 7b, the π-planes of the molecules are not parallel in the crystal. The dihedral angle for the DPH planes of A and B is 48.8(1)°. Molecules A and B have head-to-tail orientation in the crystal.

TABLE 4: Crystal Data of 1a−d

	1a[a]	**1b**[b]	**1c**[a]	**1d**[a]
formula	$C_{19}H_{17}NO_3$	$C_{20}H_{19}NO_3$	$C_{21}H_{21}NO_3$	$C_{22}H_{23}NO_3$
formula weight	307.34	321.37	335.40	349.42
crystal color, habit	yellow, plate	orange, needle	yellow, plate	orange-red, needle
crystal size (mm)	0.20 × 0.15 × 0.02		0.25 × 0.25 × 0.02	0.30 × 0.05 × 0.01
crystal system	triclinic	triclinic	monoclinic	triclinic
space group	$P\bar{1}$		$P2_1$	$P\bar{1}$
a (Å)	6.899(1)	7.16(1)	14.193(4)	8.0445(9)
b (Å)	7.223(1)	7.653(8)	7.299(2)	8.5236(9)
c (Å)	31.435(5)	16.81(5)	17.052(5)	14.171(2)
α (deg)	93.322(3)	84.1(2)	90	74.950(2)
β (deg)	93.237(3)	105.0(2)	95.895(5)	82.264(2)
γ (deg)	93.007(3)	94.32(7)	90	77.374(2)
V (Å^3)	1558.8(4)	884.6(3.1)	1757.1(9)	912.5(2)
Z	4	2	4	2
D_{calc} (g/cm^3)	1.310	1.21	1.268	1.272
T (°C)	−90	20	−90	−90
mp (°C)	184	170	160	161

[a] Obtained by single-crystal X-ray structure analysis. [b] Calculated from powder XRD pattern.

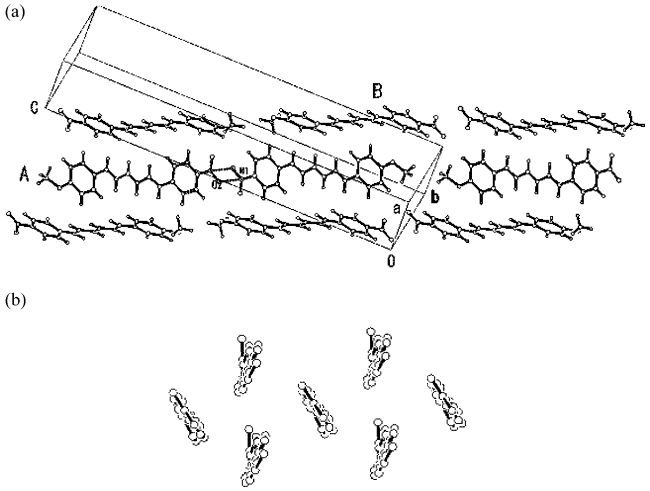

Figure 7. Crystal packing of **1a**. (a) A view from the long molecular axis. The shortest intermolecular distance between the N and O atoms is O2···N1^{i} = 2.938 (4) Å [symmetry code: (i) $-1-x$, $1-y$, $1-z$]. (b) A view from the short molecular axis.

It is noteworthy that attractive N···O dipole interactions[42] are observed between the nitro groups of the neighboring molecules of A. The shortest intermolecular distance between the N and O atoms is O2···N1^{i} = 2.938 (4) Å [symmetry code (i) $-1-x$, $1-y$, $1-z$] (Figure 7a), which is considerably short compared with those in other aromatic nitro compounds.[43]

(b) Crystal structure of **1c**. Crystal **1c** also has herringbone structure as shown in Figure 8. Two crystallographically independent molecules of A and B, whose conformations are nearly equal, exist in a unit cell. The mean deviation from the plane of DPH moiety is 0.10 Å for A and 0.15 Å for B. Thus the two molecules are basically planar. The molecular planes are not parallel in the crystal (Figure 8b). The dihedral angle for the DPH planes of A and B is 52.8(2)°. The coplanarity of molecules is low in crystal **1c**, as in the case of **1a**. The molecules A and B have head-to-tail orientation. Substantial dipole moments of **1a** and **1c** in the ground states are the cause of the head-to-tail orientation in the crystals.

The propoxy chain of molecule **1c** is not fully stretched in an all-trans conformation in the crystal (Figure 8a). The trans-gauche bent structure of the chain is likely to be a result from efficient close packing to stabilize the crystal structure.

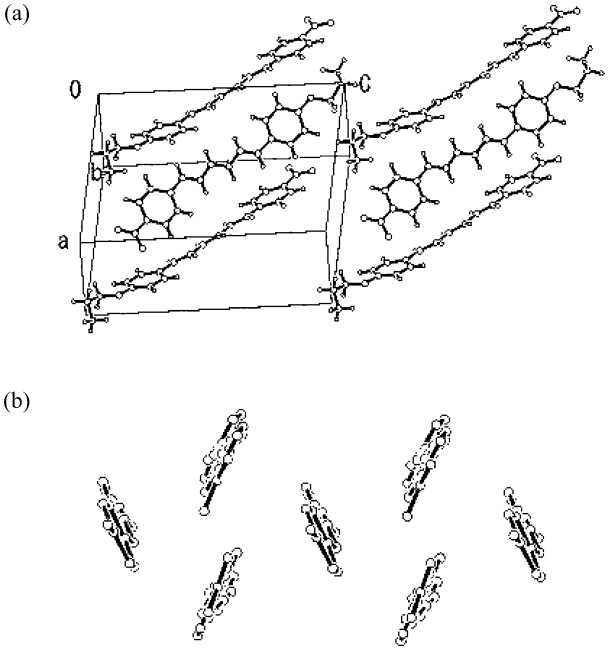

Figure 8. Crystal packing of **1c**. (a) A view from the long molecular axis. (b) A view from the short molecular axis. Molecules B (see the text) are omitted for clarity.

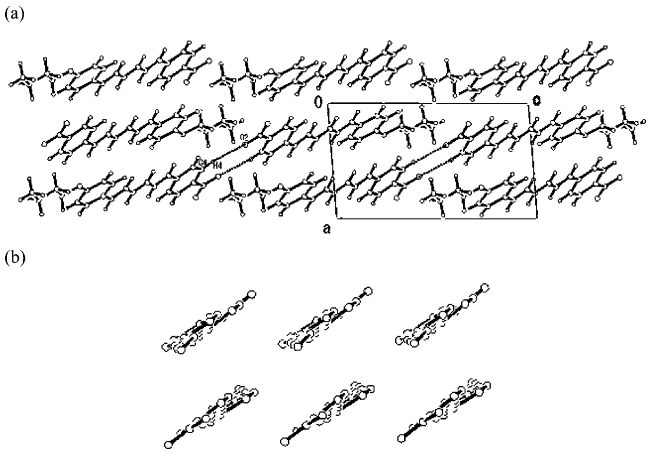

Figure 9. Crystal packing of **1d**. (a) A view from the long molecular axis. The shortest intermolecular distances between the H and O atoms and between the C and O atoms are O2···H4^{i} = 2.62 Å and O2···C4^{i} = 3.558 (2) Å [symmetry code: (i) $1-x$, $4-y$, $-1-z$], respectively, and the corresponding intermolecular angle is C4^{i}−H4^{i}···O2 =171° [symmetry code: (i) $1-x$, $4-y$, $-1-z$]. (b) A view from the short molecular axis.

(c) Crystal structure of **1d**. Crystal **1d** has π-stacked structure as shown in Figure 9. In this case, only one crystallographically independent molecule exists in a unit cell. The molecule is planar, and the mean deviation from the least-squares plane of the DPH moiety is 0.07 Å. The π-stacked neighboring molecules have antiparallel orientation.

In sharp contrast to the cases of **1a** and **1c**, the π-planes of the nearest neighboring molecules of **1d** are parallel in the crystal (Figure 9b). The dihedral angle between the DPH planes of the stacked neighbors is 0.92(2)°. Thus the molecular coplanarity is considerably high. Strong $\pi-\pi$ interaction can therefore be expected between the stacked molecules. The neighboring stacked molecules slip past each other parallel to the direction of the short molecular axis ("slipped-parallel" structure) due to the repulsion between π-electrons (Figure 9b). The slipped-parallel structure is commonly observed in the

calculated stable structures of aromatic dimers (benzene, naphthalene, and toluene)[44] and π-stacked crystals.[45]

The O atom of the nitro group is in close contact with a neighboring H atom of the nitrophenyl ring to form a weak C−H···O hydrogen bond of the type described by Desiraju and Steiner.[46,47] The H atom of the nitrophenyl ring is considered to be highly activated due to the strong electron-withdrawing nature of the nitro group, and the O atom of the nitro group is known to be a good acceptor for the C−H···O hydrogen bonds.[48] The shortest intermolecular distances between the H and O atoms and between the C and O atoms are O2···H4^{i} = 2.62 Å and O2···C4^{i} = 3.558(2) Å [symmetry code (i) $1 - x$, $4 - y$, $-1 - z$], respectively, and the corresponding intermolecular angle is C4^{i}−H4^{i}···O2 = 171° [symmetry code (i) $1 - x$, $4 - y$, $-1 - z$]. A pair of this type of hydrogen bonds makes a hexagonal space between the two nearest molecules along the long molecular axis (Figure 9a).

Chain-Length Dependence of the Crystal Structure. As described above, the crystal packing for **1a**, **1c**, and **1d** was clearly dependent on the alkoxy chain length. This is in contrast to the case of bis(alkoxycarbonyl)-substituted (*Z*,*E*,*Z*)-DPHs having alkoxy chains of different lengths, which we have recently reported.[49]

In the structures of **1a**, **1c**, and **1d**, strong crystal synthons are absent. The possible intermolecular interactions leading to crystallization, which include the $\pi-\pi$ stacking and herringbone interactions, the C−H···O hydrogen bonding, and the N···O dipole interactions, are rather weak and are in competition with each other. In such a case, the crystal packing is heavily influenced by the overall van der Waals contact and steric considerations. The chain-length dependence of the crystal structure observed for the present compounds would therefore result from the facts that the two structures, herringbone and π-stacked, are nearly isoenergetic, and that the small changes in the molecular structure (i.e., the changes in the length of the relatively short alkoxy chain) lead to the large differences in crystal packing.

Powder XRD Pattern Measurement. Powder XRD pattern measurement was performed for **1b** to obtain the cell parameters for the crystal. The powder pattern is shown in the Supporting Information, Figure S4. The parameters calculated from the pattern are listed in Table 4. The crystal system of **1b** is predicted to be triclinic, which is the same as that of **1d**. The cell parameters for **1b** are rather similar to those for **1d**. It is therefore very probable that, as in the case of **1d**, the space group of **1b** is $P\bar{1}$. If we assume this, then it is strongly suggested that the crystal of **1b** has not herringbone but π-stacked structure.

Relationship between the Solid-State Fluorescence Properties and the Crystal Structure. *Spectral Red Shifts in the Solid State.* (a) Planarization of Molecules. The absorption and fluorescence spectra for the crystals of **1a**−**d** were red-shifted relative to those for the solutions in low polar solvents.

One of the reasons for this is that the molecules are more planar in the solid state than in solution. This leads to a longer effective conjugation length of the molecules in the solid state. The DPH moieties in **1a**, **1c**, and **1d** are basically planar in the crystals. In solution, on the other hand, the phenyl groups can rotate easily. Ab initio calculations show that the torsional potential of the phenyl group is very shallow and that the about 15°-twisted structure is the most stable.

(b) Intermolecular Interactions in Crystals. Another reason for the red shifts in the solid-state spectra relative to those in solution is the stronger intermolecular interactions in crystals.

In contrast to the chain-length-independent molecular planarity in the solid state, the crystal packing is clearly dependent on the alkoxy chain length. Therefore, the red shifts in the solid-state fluorescence of **1b** and **1d** relative to the emission of **1a** and **1c** should be attributed to the differences in the type and strength of intermolecular interactions in crystals.

The strong $\pi-\pi$ interaction between the stacked molecules of **1d** in the crystal leads to large red shifts in the solid-state spectra. In the crystals of **1a** and **1c**, on the other hand, the $\pi-\pi$ intermolecular interaction between the neighboring molecules is weak due to their herringbone structure. Considering that the π-stacked structure is strongly suggested for **1b**, it can safely be said that the spectral red shifts in the solid state relative to those in solution are larger for the crystals with π-stacked structure than for the crystals with herringbone structure.

It should be noted that, although the C−H···O hydrogen bonds are weak in nature, the multiple hydrogen bonds in crystal **1d** may possibly lead to the red shift in its solid-state fluorescence spectrum to some extent.

In the solid state, the "polarity" experienced by molecules increases as a consequence of intermolecular interactions. Different from the observations in polar solvents, however, TICT did not take place during the photoprocesses of **1a**−**d** in the crystalline state. This is probably because the bond twisting which is required by the formation of TICT state is difficult to produce in the rigid crystal lattice. For the TICT state formation of *p*-nitro-substituted diphenylpolyenes in solution, the twisting of the C−N single bond between the nitro and the phenyl groups is suggested.[31,50]

Monomeric Origin of the Solid-State Fluorescence. In the crystals of **1a** and **1c**, the π-planes of the neighboring molecules are not parallel. The low coplanarity of molecule prevents the formation of an excimer, leading to the monomer emission.

In contrast, the π-planes of the neighboring molecules are all parallel in the crystal of **1d**. The excimer formation can therefore be expected. In fact, however, the observed fluorescence was shown to be derived from monomeric species, although the strong $\pi-\pi$ interaction induced significant red shifts in the solid-state spectra. This can be attributed to the limited overlap between the molecular π-planes in the slipped-parallel structure. The excimer formation requires strong orbital−orbital interaction, and the magnitude of the interaction depends critically on the molecular orientation. No observation of excimer fluorescence is considered to be due to the unsuitable molecular orientation in the crystal of **1d**.

It is interesting to compare the present results with our earlier observation that *p*,*p*′-diformyl-substituted (*E*,*E*,*E*)-DPH exhibits excimer fluorescence in the solid state.[28] Although its crystal structure is unknown, the formation of a [2 + 2] mirror symmetric photodimer strongly suggests the existence of a parallel-aligned face-to-face pair in the crystal.[51,52] This is in contrast to the fact that crystal **1d**, despite having π-stacked structure, was photostable and showed no excimer emission. Again these indicate that the relative orientation of the interacting two molecules is of great importance for the formation of excimer in these polyenes.

Conclusions

The fluorescence spectra for the crystals of **1a**−**d** were red-shifted relative to those for the solutions in low polar solvents. This can be attributed to the planarization of molecules in the solid state, and to the strong intermolecular interactions in crystals. The fluorescence maxima for the crystals of **1b** and **1d** were observed at longer wavelengths than those for **1a** and

1c. The chain-length dependence of the solid-state emission spectra is mainly due to the differences in crystal packing. It is very probable that the spectral red shifts in the solid state relative to those in solution are larger for the crystals with π-stacked structure than for the crystals with herringbone structure. For all compounds studied, the solid-state emission was shown to be originated not from an excimer or molecular aggregated complexes but from only one emitting monomeric species. Although the strong $\pi-\pi$ interaction between the stacked molecules of **1d** in the crystal led to significantly large red shifts in the solid-state spectra, the excimer formation was prevented by the limited overlap between the molecular π-planes due to the slipped-parallel structure.

Acknowledgment. We thank Dr. Y. Kawanishi (AIST) for the use of his fluorescence spectrometer.

Supporting Information Available: Crystallographic data for **1a**, **1c**, and **1d** in CIF format; preparation procedures and spectroscopic data for **3** and **4**; crystal and structure refinement data for **1a**, **1c**, and **1d**; ORTEP representations for the molecular structures of **1a**, **1c**, and **1d**; powder XRD pattern of **1b**; results of quantum chemical calculations for **1a**. This material is available free of charge via the Internet at http://pubs.acs.org.

References and Notes

(1) (a) Kraft, A.: Grimsdale, A. C.; Holmes, A. B. *Angew. Chem., Int. Ed.* **1998**, *37*, 402. (b) Heeger, A. J. *Solid State Commun.* **1998**, *107*, 673. (c) Friend, R. H.; Gymer, R. W.; Holmes, A. B.; Burroughes, J. H.; Marks, R. N.; Talliani, C.; Bradley, D. D. C.; Dos Santos, D. A.; Brédas, J. L.; Lögdlund, M.; Salaneck, W. R. *Nature (London)* **1999**, *397*, 121. (d) Bernius, M. T.; Inbasekaran, M.; O'Brien, J.; Wu, W. *Adv. Mater.* **2000**, *12*, 1737.

(2) Van Hutten, P. F.; Krasnikov, V. V.; Hadziioannou, G. *Acc. Chem. Res.* **1999**, *32*, 257.

(3) (a) Oelkrug, D.; Tompert, A.; Gierschner, J.; Egelhaaf, H.-J.; Hanack, M.; Hohloch, M.; Steinhuber, E. *J. Phys. Chem. B* **1998**, *102*, 1902. (b) Strehmel, B.; Sarker, A. M.; Malpert, J. H.; Strehmel, V.; Seifert, H.; Neckers, D. C. *J. Am. Chem. Soc.* **1999**, *121*, 1226.

(4) (a) Wu, C. C.; DeLong, M. C.; Vardeny, Z. V.; Ferraris, J. P. *Synth. Met.* **2003**, *137*, 939. (b) Lim, S.-H.; Bjorklund, T. G.; Bardeen, C. J. *J. Phys. Chem. B* **2004**, *108*, 4289. (c) Bhongale, C. J.; Chang, C.-W.; Lee, C.-S. Diau, E. W.-G.; Hsu, C.-S. *J. Phys. Chem. B* **2005**, *109*, 13472.

(5) Xie, Z.; Yang, B.; Li, F.; Cheng, G.; Liu, L.; Yang, G.; Xu, H.; Ye, L.; Hanif, M.; Liu, S.; Ma, D.; Ma, Y. *J. Am. Chem. Soc.* **2005**, *127*, 14152.

(6) Niazimbetova, Z. I.; Christian, H. Y.; Bhandari, Y. J.; Beyer, F. L. Galvin, M. E. *J. Phys. Chem. B* **2004**, *108*, 8673.

(7) Wilson, J. N.; Smith, M. D.; Enkelmann, V.; Bunz, U. H. F. *Chem. Commun.* **2004**, 1700.

(8) (a) Domercq, B.; Grasso, C.; Maldonado, J.-L.; Halik, M.; Barlow, S.; Marder, S. R.; Kippelen, B. *J. Phys. Chem. B* **2004**, *108*, 8647. (b) Wu, F.-I.; Shih, P.-I.; Tseng, Y.-H.; Chen, G.-Y.; Chien, C.-H.; Shu, C.-F.; Tung, Y.-L.; Chi, Y.; Jen, A. K.-Y. *J. Phys. Chem. B* **2005**, *109*, 14000. (c) Chen, X.; Tseng, H.-E.; Liao, J.-L.; Chen, S.-A. *J. Phys. Chem. B* **2005**, *109*, 17496. (d) Hung, M.-C.; Liao, J.-L.; Chen, S.-A.; Chen, S.-H.; Su, A.-C. *J. Am. Chem. Soc.* **2005**, *127*, 14576.

(9) Kulkarni, A. P.; Kong, X.; Jenekhe, S. A. *J. Phys. Chem. B* **2004**, *108*, 8689.

(10) Wolak, M. A.; Jang, B.-B.; Palilis, L. C.; Kafafi, Z. H. *J. Phys. Chem. B* **2004**, *108*, 5492.

(11) (a) de Halleux, V.; Calbert, J.-P.; Brocorens, P.; Cornil, J.; Declercq, J.-P.; Brédas, J.-L.; Geerts, Y. *Adv. Funct. Mater.* **2004**, *14*, 649. (b) Qu, L.; Shi, G. *Chem. Commun.* **2004**, 2800. (c) Hayer, A.; de Halleux, V.; Köhler, A.; El-Garoughy, A.; Meijer, E. W.; Barberá, J.; Tant, J.; Levin, J.; Lehmann, M.; Gierschner, J.; Cornil, J.; Geerts Y. H. *J. Phys. Chem. B* **2006**, *110*, 7653.

(12) (a) Shi, M.-M.; Chen, H.-Z.; Shi, Y.-W.; Sun, J.-Z.; Wang, M. *J. Phys. Chem. B* **2004**, *108*, 5901. (b) Zhang, H.; Yang, B.; Zheng, Y.; Yang, G.; Ye, L.; Ma, Y.; Chen, X.; Cheng, G.; Liu, S. *J. Phys. Chem. B* **2004**, *108*, 9571. (c) Ferrer, M. L.; del Monte, F. *J. Phys. Chem. B* **2005**, *109*, 80. (d) Gong, J.-R.; Wan, L.-J.; Lei, S.-B.; Bai, C.-L.; Zhang, X.-H.; Lee, S.-T. *J. Phys. Chem. B* **2005**, *109*, 1675. (e) Sakuda, E.; Tsuge, K.; Sasaki, Y.; Kitamura, N. *J. Phys. Chem. B* **2005**, *109*, 22326. (f) Tonzola, C. J.; Hancock, J. M.; Babel, A.; Jenekhe, S. A. *Chem. Commun.* **2005**, 5214. (g) Tong, H.; Dong, Y.; Häussler, M.; Lam, J. W. Y.; Sung, H. H.-Y.; Williams, I. D.; Sun, J.; Tang, B. Z. *Chem. Commun.* **2006**, 1133.

(13) Kim, Y.; Bouffard, J.; Kooi, S. E.; Swager, T. M. *J. Am. Chem. Soc.* **2005**, *127*, 13726.

(14) Singh, A. K.; Kanvah, S. *Indian J. Chem., Sect. B* **2001**, *40*, 965.

(15) Davis, R.; Rath, N. P.; Das, S. *Chem. Commun.* **2004**, 74.

(16) Kasha, M. *Radiat. Res.* **1963**, *20*, 55.

(17) Davis, R.; Abraham, S.; Rath, N. P.; Das, S. *New J. Chem.* **2004**, *28*, 1368.

(18) Ortiz, A.; Flora, W. H.; D'Ambruoso, G. D.; Armstrong, N. R.; McGrath, D. V. *Chem. Commun.* **2005**, 444.

(19) Chiang, C.-L.; Wu, M.-F.; Dai, D.-C.; Wen, Y.-S.; Wang, J.-K.; Chen, C.-T. *Adv. Funct. Mater.* **2005**, *15*, 231.

(20) (a) Mizobe, Y.; Tohnai, N.; Miyata, M.; Hasegawa, Y. *Chem. Commun.* **2005**, 1839. (b) Mizobe, Y.; Ito, H.; Hisaki, I.; Miyata, M.; Hasegawa, Y.; Tohnai, N. *Chem. Commun.* **2006**, 2126.

(21) (a) Thomas, K. R. J.; Lin, J. T.; Velusamy, M.; Tao, Y.-T.; Chuen, C.-H. *Adv. Funct. Mater.* **2004**, *14*, 83. (b) Sun, X.; Liu, Y.; Xu, X.; Yang, C.; Yu, G.; Chen, S.; Zhao, Z.; Qiu, W.; Li, Y.; Zhu, D. *J. Phys. Chem. B* **2005**, *109*, 10786.

(22) (a) Islam, A.; Cheng, C.-C.; Chi, S.-H.; Lee, S. J.; Hela, P. G.; Chen, I.-C.; Cheng, C.-H. *J. Phys. Chem. B* **2005**, *109*, 5509. (b) Ho, T.-I.; Elangovan, A.; Hsu, H.-Y.; Yang, S.-W. *J. Phys. Chem. B* **2005**, *109*, 8626. (c) Kulkarni, A. P.; Wu, P.-T.; Kwon, T. W.; Jenekhe, S. A. *J. Phys. Chem. B* **2005**, *109*, 19584.

(23) (a) Lin, C. T.; Guan, H. W.; McCoy, R. K.; Spangler, C. W. *J. Phys. Chem.* **1989**, *93*, 39. (b) Viallet, J.-M.; Dupuy, F.; Lapouyade, R.; Rullière, C. *Chem. Phys. Lett.* **1994**, *222*, 571.

(24) (a) Singh, A. K.; Kanvah, S. *New J. Chem.* **2000**, *24*, 639. (b) Davis, R.; Das, S.; George, M.; Druzhinin, S.; Zachariasse, K. A. *J. Phys. Chem. A* **2001**, *105*, 4790. (c) El-Gezawy, H.; Rettig, W.; Lapouyade, R. *J. Phys. Chem. A* **2006**, *110*, 67.

(25) Görner, H. *Ber. Bunsen-Ges. Phys. Chem.* **1998**, *102*, 726.

(26) (a) Sumalekshmy, S.; Gopidas, K. R. *J. Phys. Chem. B* **2004**, *108*, 3705. (b) Elangovan, A.; Kao, K.-M.; Yang, S.-W.; Chen, Y.-L.; Ho, T.-I.; Su, Y. O. *J. Org. Chem.* **2005**, *70*, 4460. (c) Ihmels, H.; Meiswinkel, A.; Mohrschladt, C. J.; Otto, D.; Waidelich, M.; Towler, M.; White, R.; Albrecht, M.; Schnurpfeil, A. *J. Org. Chem.* **2005**, *70*, 3929. (d) Yamaguchi, Y.; Ochi, T.; Wakamiya, T.; Matsubara, Y.; Yoshida, Z.-I. *Org. Lett.* **2006**, *8*, 717.

(27) Vaday, S.; Geiger, H. C.; Cleary, B.; Perlstein, J.; Whitten, D. G. *J. Phys. Chem. B* **1997**, *101*, 321.

(28) Sonoda, Y.; Kawanishi, Y.; Ikeda, T.; Goto, M.; Hayashi, S.; Yoshida, Y.; Tanigaki, N.; Yase, K. *J. Phys. Chem. B* **2003**, *107*, 3376.

(29) Sonoda, Y.; Kawanishi, Y. *Chem. Lett.* **2003**, *32*, 978.

(30) Lin, Y. R.; Hong, Y.-L. V.; Hong, J.-L. *Mol. Cryst. Liq. Cryst. A* **1994**, *241*, 69.

(31) Sonoda, Y.; Kwok, W. M.; Petrasek, Z.; Ostler, R.; Matousek, P.; Towrie, M.; Parker, A. W.; Phillips, D. *J. Chem. Soc., Perkin Trans. 2* **2001**, 308.

(32) Birks, J. B.; Kazzaz, A. A.; King, T. A. *Proc. R. Soc.* **1966**, *A291*, 556.

(33) *SMART*, Version 5.625; Bruker AXS: Madison, WI, 2001. *SAINT-PLUS*, Version 6.22; Bruker AXS: Madison, WI, 2001. Sheldrick, G. M. *SADABS, Program for scaling and correction of area, detector data*; University of Göttingen: Germany, 1998.

(34) Altomare, A.; Cascarano, G.; Giacovazzo, C.; Guagliardi, A.; Brula, M. C.; Polidori, G.; Camalli, M. *J. Appl. Crystallogr.* **1994**, *27*, 435.

(35) Sheldrick, G. M. *SHELXTL*, Version 6.12; Bruker AXS: Madison, WI, 2000.

(36) Frisch, M. J.; Trucks, G. W.; Schlegel, H. B.; Scuseria, G. E.; Robb, M. A.; Cheeseman, J. R.; Montgomery, J. A., Jr.; Vreven, T.; Kudin, K. N.; Burant, J. C.; Millam, J. M.; Iyengar, S. S.; Tomasi, J.; Barone, V.; Mennucci, B.; Cossi, M.; Scalmani, G.; Rega, N.; Petersson, G. A.; Nakatsuji, H.; Hada, M.; Ehara, M.; Toyota, K.; Fukuda, R.; Hasegawa, J.; Ishida, M.; Nakajima, T.; Honda, Y.; Kitao, O.; Nakai, H.; Klene, M.; Li, X.; Knox, J. E.; Hratchian, H. P.; Cross, J. B.; Bakken, V.; Adamo, C.; Jaramillo, J.; Gomperts, R.; Stratmann, R. E.; Yazyev, O.; Austin, A. J.; Cammi, R.; Pomelli, C.; Ochterski, J. W.; Ayala, P. Y.; Morokuma, K.; Voth, G. A.; Salvador, P.; Dannenberg, J. J.; Zakrzewski, V. G.; Dapprich, S.; Daniels, A. D.; Strain, M. C.; Farkas, O.; Malick, D. K.; Rabuck, A. D.; Raghavachari, K.; Foresman, J. B.; Ortiz, J. V.; Cui, Q.; Baboul, A. G.; Clifford, S.; Cioslowski, J.; Stefanov, B. B.; Liu, G.; Liashenko, A.; Piskorz, P.; Komaromi, I.; Martin, R. L.; Fox, D. J.; Keith, T.; Al-Laham, M. A.; Peng, C. Y.; Nanayakkara, A.; Challacombe, M.; Gill, P. M. W.; Johnson, B.; Chen, W.; Wong, M. W.; Gonzalez, C.; Pople, J. A. *Gaussian 03*, revision C.02; Gaussian, Inc.: Wallingford, CT, 2004.

(37) Foresman, J. B.; Head-Gordon, M.; Pople, J. A.; Frisch, M. J. *J. Phys. Chem.* **1992**, *96*, 135.

(38) Lee, C.; Yang, W.; Parr, R. G. *Phys. Rev. B* **1988**, *37*, 785.

(39) Becke, A. D. *J. Chem. Phys.* **1993**, *98*, 5648.

(40) Grabowski, Z. R.; Rotkiewicz, K.; Rettig, W. *Chem. Rev.* **2003**, *103*, 3899.

(41) Jenekhe, S. A.; Osaheni, J. A. *Science* **1994**, *265*, 765.

(42) (a) Wozniak, K.; He, H.; Klinowski, J.; Jones, W.; Grech, E. *J. Phys. Chem.* **1994**, *98*, 13755. (b) Platts, J. A.; Howard, S. T.; Wozniak, K. *Chem. Phys. Lett.* **1995**, *232*, 479. (c) Wozniak, K.; Mallinson, P. R.; Wilson, C. C.; Hovestreydt, E.; Grech, E. *J. Phys. Chem. A* **2002**, *106*, 6897. (d) Paulini, R.; Muller, K.; Diederich, F. *Angew. Chem., Int. Ed.* **2005**, *44*, 1788.

(43) For the examples of the very short N···O distances in nitro aromatics, see: (a) Zeller, M.; Hunter, A. D. *Acta Crystallogr.* **2004**, *C60*, o415. (b) Sonoda, Y.; Kawanishi, Y.; Goto, M. *Acta Crystallogr.* **2005**, *E61*, o1200.

(44) (a) Hobza, P.; Selzle, H. L.; Schlag, E. W. *J. Am. Chem. Soc.* **1994**, *116*, 3500. (b) Tsuzuki, S.; Honda, K.; Uchimaru, T.; Mikami, M. *J. Chem. Phys.* **2004**, *120*, 647. (c) Tsuzuki, S.; Honda, K.; Uchimaru, T.; Mikami, M. *J. Chem. Phys.* **2005**, *122*, 144323.

(45) (a) Desiraju, G. R.; Gavezzotti, A. *J. Chem. Soc., Chem. Commun.* **1989**, 621. (b) Tsuzuki, S.; Honda, K.; Azumi, R. *J. Am. Chem. Soc.* **2002**, *124*, 12200.

(46) Desiraju, G. R.; Steiner, T. *The Weak Hydrogen Bond in Structural Chemistry and Biology*; Oxford University Press: New York, 1999.

(47) (a) Desiraju, G. R. *Acc. Chem. Res.* **1991**, *24*, 290. (b) Desiraju, G. R. *Acc. Chem. Res.* **1996**, *29*, 441. (c) Desiraju, G. R. *Chem. Commun.* **2005**, 2995.

(48) (a) Sharma, C. V. K.; Desiraju, G. R. *J. Chem. Soc., Perkin Trans. 2* **1994**, 2345. (b) Thaimattam, R.; Xue, F.; Sarma, J. A. R. P.; Mak, T. C. W.; Desiraju, G. R. *J. Am. Chem. Soc.* **2001**, *123*, 4432.

(49) Sonoda, Y.; Kawanishi, Y.; Tsuzuki, S.; Goto, M. *J. Org. Chem.* **2005**, *70*, 9755.

(50) Singh, A. K.; Darshi, M.; Kanvah, S. *New J. Chem.* **1999**, *23*, 1075.

(51) Sonoda, Y.; Miyazawa, A.; Hayashi, S.; Sakuragi, M. *Chem. Lett.* **2001**, 410.

(52) For the diformyl derivative, the face-to-face molecular arrangement in the solid state is consistent with the results from two-dimensional ^{1}H spin-exchange NMR study. Hayashi, S.; Sonoda, Y. *Bull. Chem. Soc. Jpn.* **2004**, *77*, 2159.